COMPUTER METHODS AND PROGRAMS IN BIOMEDICINE 107 (2012) 490–496

journal homepage: www.intl.elsevierhealth.com/journals/cmpb

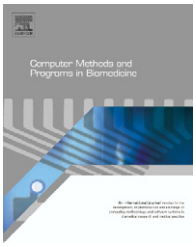

QRS detection based on wavelet coefficients

Zahia Zidelmal[a], *Ahmed Amirou*[a], *Mourad Adnane*[b,*], *Adel Belouchrani*[b]

[a] *Electrical Engineering Department, Mouloud Mammeri University, Tizi-Ouzou, Algeria*
[b] *Electrical Engineering Department, Ecole Nationale Polytechnique, Algiers, Algeria*

ARTICLE INFO

Article history:
Received 27 July 2011
Received in revised form
17 November 2011
Accepted 7 December 2011

Keywords:
QRS detection
Power spectrum
Wavelet detail coefficients

ABSTRACT

Electrocardiogram (ECG) signal processing and analysis provide crucial information about functional status of the heart. The QRS complex represents the most important component within the ECG signal. Its detection is the first step of all kinds of automatic feature extraction. QRS detector must be able to detect a large number of different QRS morphologies. This paper examines the use of wavelet detail coefficients for the accurate detection of different QRS morphologies in ECG. Our method is based on the power spectrum of QRS complexes in different energy levels since it differs from normal beats to abnormal ones. This property is used to discriminate between true beats (normal and abnormal) and false beats. Significant performance enhancement is observed when the proposed approach is tested with the MIT-BIH arrhythmia database (MITDB). The obtained results show a sensitivity of 99.64% and a positive predictivity of 99.82%.

1. Introduction

The electrocardiogram (ECG) is a signal that records the electrical activity of the heart. The ECG waveform is characterized by its main waves: P, QRS and T (see Fig. 1). The most important wave is the QRS complex characterizing the ventricular contractions. Since ECG reflects the rhythmic electrical depolarization and repolarization of the atria and ventricles, its shape, time interval and amplitude provide useful informations about the current state of the heart. QRS detection is the first step of all kinds of automatic feature extraction. Accurate detection of QRS is an important issue in many clinical conditions. The QRS complex is the dominant feature of the ECG signal and its detection can be done rather easily by the trained eye of a cardiologist. Unluckily, the problem of automation of this process is not simple due to the fact that morphologies of many normal as well as abnormal QRS complexes differ widely. The presence of noise from many sources makes this problem more complex. Further, other sections of ECG (P and T waves) can hinder the detection of QRS complexes.

QRS detection has been a research topic for more than 30 years. A wide diversity of algorithms has been proposed in the literature, for an extensive review, see [1]. The slope of the R wave is a popular signal feature used to locate the QRS complex in many QRS detectors. Such algorithms are based on signal derivative [2–4]. However, a derivative amplifies the undesirable higher frequency noise components. Also, many abnormal QRS complexes with large amplitudes and long durations such as ectopic ones are missed in a purely derivative approach because of their relatively low R wave slopes. To achieve reliable performance, we must extract other parameters from the signal such as morphology, width, and frequency component. Other algorithms based on more sophisticated digital filters and irregular RR intervals checkup strategy are published in [5]. Within the last two decades, new approaches to QRS detection have been proposed e.g. algorithms based on artificial neural networks [6,7], genetic algorithms [8]. Among

* *Corresponding author.*
E-mail addresses: z-zidelmal@mail.ummto.dz (Z. Zidelmal), a-amirou@mail.ummto.dz (A. Amirou), mourad.adnane@enp.edu.dz (M. Adnane), adel.belouchrani@enp.edu.dz (A. Belouchrani).
0169-2607/$ – see front matter © 2011 Elsevier Ireland Ltd. All rights reserved.
doi:10.1016/j.cmpb.2011.12.004

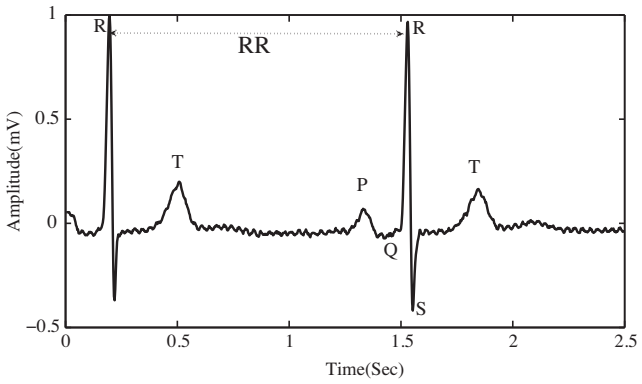

Fig. 1 – The QRS complex within the ECG signal.

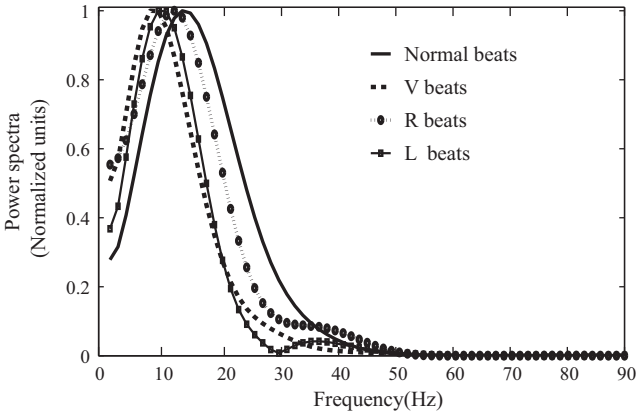

Fig. 2 – Power spectra of four QRS types.

all these methods, wavelet analysis is a promising mathematical tool that gives good estimation of time frequency localization and provides flexibility and adaptability. A number of techniques have been attempted to use wavelets for QRS complex detection e.g. [9] where the authors illustrate multi resolution analysis using Dyadic wavelet Transform and [10] examining the choice of wavelet functions to determine the effects of wavelet properties such as linearity and time-frequency localization on the accuracy of QRS detection.

Robustness and high detection accuracy still remain open problems. Note that for all algorithms, detection errors occur mainly at beats with decreased signal slope, such as ectopic beats [1]. In this paper, we exploit our knowledge of different beat features to detect QRS waves. We propose a method based on wavelet detail coefficients. After a preliminary investigation of QRS spectral parameters, wavelet detail coefficients d_4 and d_5 containing respectively the highest energy of normal beats and abnormal beats are used. The proposed algorithm is tested with respect to the MIT-BIH arrhythmia database (MITDB). The obtained results show a sensitivity of 99.64% and a positive predictivity of 99.82%. The paper is organized as follows. Section 2 presents the investigation of energy levels of normal and abnormal ECG beats. Accordingly, an algorithm of R peak detection is developed. The proposed method is tested in Section 3. Finally, Section 4 concludes the paper.

2. Method

2.1. MIT-BIH arrhythmia database

The annotated ECG records from the MIT-BIH arrhythmia database [11] have been used in this study. This database has 48 records. Each record is of 30 min length with 360 Hz sampling frequency. Each record consists of the upper and lower leads. Since normal QRS complexes might be usually prominent in the upper lead, the upper lead was used as a default.

The ECG records present a variety of waveforms, artifacts, complex ventricular, junctional and supraventricular arrhythmias and conduction abnormalities. Each tape is accompanied by an annotation file in which each ECG beat has been identified by expert cardiologists. These labels, referred to as 'truth' annotation and are used to evaluate the performance of our detector.

2.2. Power spectrum of the QRS complex

To study the QRS frequency content, four heartbeat types are considered: normal beats (N), ventricular extra-systoles (V), left and right bundle branch blocks (L and R). Such beats represent predominant classes in all records. Each heartbeat type was represented by 200 beats selected from all ECG recordings. The QRS complex was extracted within a fixed-length window around the fiducial point (annotated time), starting about 50 ms before and ending about 130 ms after. The QRS window contains 64 samples (18 before, 46 after) for sampling rate of 360 Hz. For each QRS complex, the power spectrum is processed by Fast Fourier Transform (FFT). Before computing FFT, the segment containing the QRS is multiplied with a Blackman window to force the beginning and the end of the segment to 0. Thus, to suppress discontinuities due to possible adjacent P and T waves. Blackman's window is also selected as it gives maximum side lobe attenuation (−74 dB) in the frequency domain and has a moderately wide main lobe. The power spectra of these QRS classes is displayed in Fig. 2.

We can see in Fig. 2 that the spectra of V, L and R beats distinguish from the spectra of N beats at all power levels due to changes in the rhythm origination and the conduction paths and therefore progressing more slowly.

2.3. Discrete wavelet transform

Discrete wavelet transform decomposes a signal at different scales. Filters of different cut-off frequencies are used for analyzing the signal at different resolution levels. For this purpose, the signal is passed through series of high pass and low pass filters in order to analyze low as well as high frequencies in the signal. At each level, the high pass filter produces detail information d_n, while the low pass filter associated with scaling function produces coarse approximations A_n. The half band filters produce signals spanning only half the frequency band. This doubles the frequency resolution. In accordance with Nyquist's rule, if the original signal has a highest frequency f_{max}, it requires a sampling frequency $f_s = 2f_{max}$. Hence, at each decomposition level j, the frequency axis is recursively divided into halves at the ideal cut-off frequencies $f_j = f_s/2^{j+1}$.

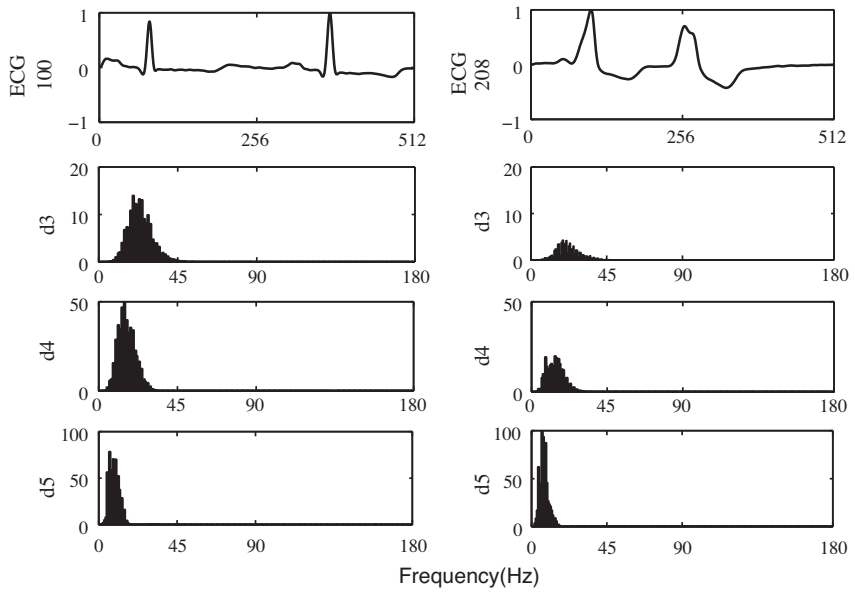

Fig. 3 – Energy levels of N beats (left) and for V beats (right). For comparison, the same scale is used at each level.

2.3.1. *Wavelet selection*

The selection of relevant wavelet is an important task before starting the detection procedure. But there is no universal method suggested to select a particular wavelet. The choice of wavelet depends upon the type of signal to be analyzed and the application. There are several wavelet families like Haar, Daubechies, Biorthogonal, Coiflets, Symlets, Morlet, Mexican Hat, Meyer. However, Haar wavelet has been found to give details more accurately than other wavelets. The Haar wavelet is compact and provides localization in time.

2.4. *ECG decomposition*

The signal under test is decomposed up to a desired level depending upon dominant frequency components in the signal. The choice of desired level of decomposition is dependent on required frequency components available in the wavelet coefficient at that level. The ECG records taken from the MIT-BIH arrhythmia database are sampled at 360 Hz. In accordance with Nyquist's rule, the range of real frequency components of the signals is between 0 and 180 Hz. The correspondence between the details and range of frequencies is given in Table 1.

Table 1 – Correspondence between details and range frequencies.

Detail	Frequency range
d_1	90 Hz, . . . , 180 Hz
d_2	45 Hz, . . . , 90 Hz
d_3	22.5 Hz, . . . , 45 Hz
d_4	11.25 Hz, . . . , 22.5 Hz
d_5	5.62 Hz, . . . , 11.25 Hz

2.4.1. *Selection of detail coefficients*

Most of the energy of ECG signal is concentrated within the QRS complex [12]. According to Table 1 and considering Fig. 2 showing that the energy of both normal and abnormal beats is concentrated between 5 Hz and 22 Hz, the signal is decomposed until level 5. To investigate the energy levels of normal and abnormal beats, a segment containing two normal beats (highest frequencies) was kept from record 100 and a segment containing V beats (lowest frequencies) is kept from record 208.

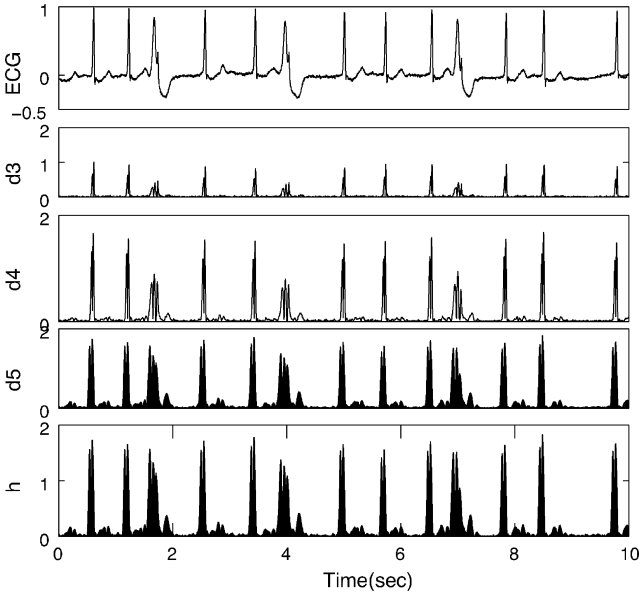

Fig. 4 – Decomposition of ECG signal using 'Haar' wavelet for record 221. Although the original signal is of 30 min duration, for better illustration details are scaled and signal is shown for 10 s duration only.

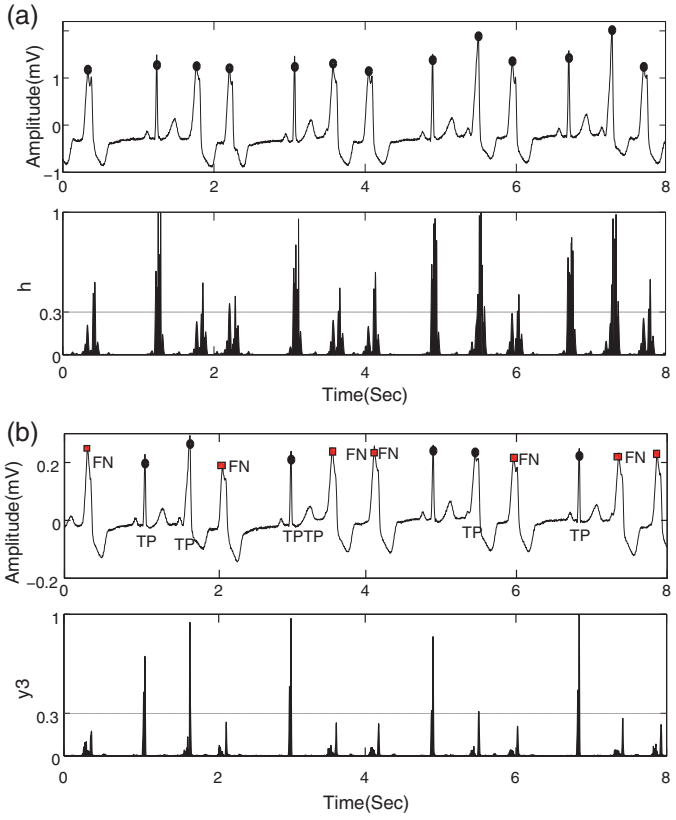

Fig. 5 – Comparison between our method (a) and Tompkins algorithm (b). The bullets represent R peak positions detected where the rectangles represent undetected beats; y3 is the squared second derivative of ECG signal [2].

For each level, the power spectrum (based on the FFT) of a set of 512 sample points corresponding approximately to two heartbeats is processed. In each segment, the peak of the frequency spectrum obtained corresponds to the peak energy of the QRS complex. The energy content for the decomposed levels of records 100 and 208 is shown in Fig. 3. Details d_1 and d_2 are not represented since they are out of range of QRS

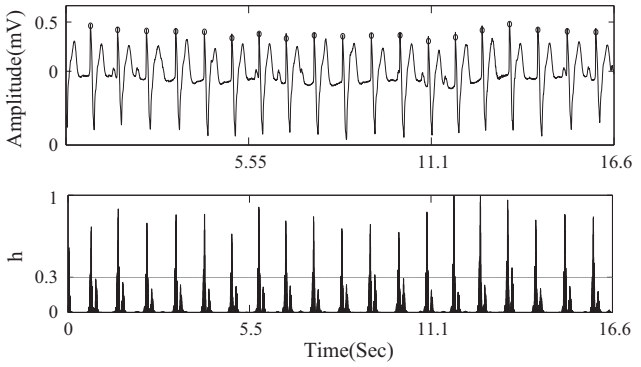

Fig. 6 – Plots of ECG waveforms and R peaks localization for MITDB record. 107: 0–16 s, the bullets represent R peak positions detected.

frequencies. The energy plot (Fig. 3) shows that QRS energy is highest at level 4 for N beats while for V beats, the energy is highest at level 5. Accordingly, the details selected are d_4 and d_5. Hence, the effect of baseline shift, T and P waves having a frequency range of [0 Hz, . . ., 5 Hz] is eliminated. The product of the selected details is processed and used to localize QRS complexes (see Fig. 4). The following algorithm summarizes the procedure used for detecting R peak localization through Haar wavelet coefficients:

1 Apply Haar wavelet transform to ECG signal $x(i)$,
2 Compute the product $h = \mid \prod_{j=4}^{5} d_j \mid$,
3 QRS localization: select $h(i)$ associated to QRS complex using a threshold $\lambda = 0, 3 * \max(h)$,
   - if $h(i) \geq \lambda$ then position i⇒ QRS (candidate),
   - else position i⇒ Not QRS,
4 Identify different QRS complexes: if i, i′ are consecutive selected positions: $|i - i'| < 36$ then i, i′⇒ same QRS-else i, i′ ⇒ Not same QRS. ($36 * f_s = 100$ ms is the standard QRS duration),
5 Elimination of multiple detection: a peak occurring within the refractory period (200 ms) is disregarded. This constraint is a physiological one due to the refractory period during which ventricular depolarization cannot occur,

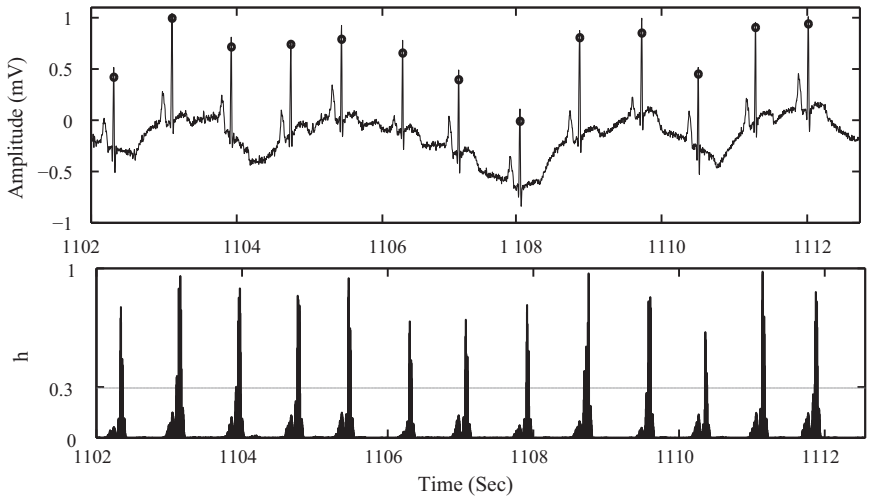

Fig. 7 – Plots of ECG waveforms and R peaks localization for MITDB record. 222: 1102–1112 s presenting a baseline shift.

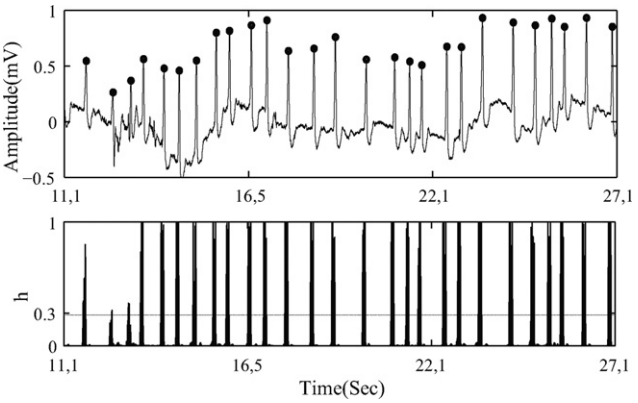

Fig. 8 – ECG waveforms and R peaks localization for record 203 (11.1–27.1 s).

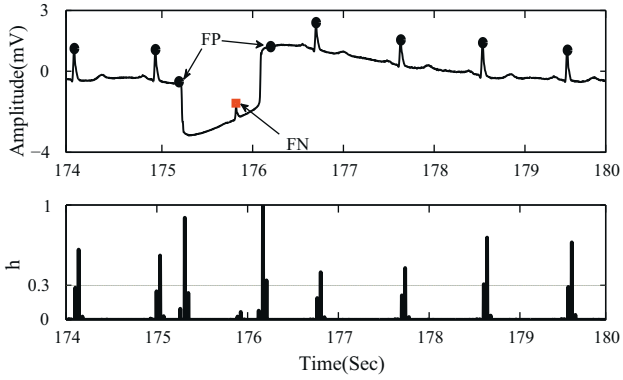

Fig. 10 – Plots of ECG waveforms and R peaks localization for MITDB record. 101: 174–180 s with severe abrupt change in potential.

6 Searchback for missed QRS complexes: If no QRS complex is detected within 150% of the current RR interval, then we apply a searchback using a secondary threshold of 0.5 times the previous one for the intervening time segment to find any missed peaks. This segment value was used in [3,4] and has a physiological origin: the time value between adjacent heartbeats cannot change more quickly than this.

3. Evaluation results and discussions

For the analysis of detector performance, it is necessary to use a standard database so obtained results can be interpreted and compared to other results with respect to that manually annotated database. The complete database was analyzed, except for record 207; Ventricular Flutter (VF) intervals for a total of 142.5 s are excluded. Note that these intervals are not annotated.

For comparison, we apply our method and the well known Tompkins algorithm [2] to a segment of record 208 (0 s, . . ., 8 s) presenting normal beats and wide ectopic beats. Fig. 5a shows that our algorithm detects all R peaks with only the initial threshold $\lambda = 0, 3 * \max(h)$, However when we use the detection strategy [2], the derivative amplifies the higher frequencies characteristic of the N beats while attenuating the lower frequencies of V beats needing a search back detections and other threshold values in the decision-making (Fig. 5b).

To illustrate the effectiveness of R peak localization, we select some ECG segments with complicated patterns. Fig. 6 represents a segment of record 107 (0–16 s) containing paced beats. The R peaks are correctly localized even though tall T waves succeeding them because the effect of T waves is eliminated.

Baseline drift having a frequency range of (0 Hz, . . ., 2.5 Hz) [12] is completely eliminated in the signal h. This is shown in Fig. 7 representing a segment of record 222 (1102–1112 s).

Record 203 (Fig. 8) presents ectopic beats with variable RR intervals and sudden R amplitude variation. R peak positions are correctly detected with a unique threshold λ.

ECG signal with severe muscle artifacts is given in Fig. 9. Even though the amplitude of these artifacts, one can see that they are easily eliminated considering d_4 and d_5. The artifacts in the segment (319–320 s) are higher than the R wave but significantly attenuated in the resultant signal h.

ECG waveforms for the records 101 (174–180 s) is a case of severe abrupt change in potential leading to higher detail coefficients in the corresponding positions. In this segment two false positive beats (*FP*) and one false negative (*FN*) are identified (Fig. 10). ECG segment from record 203 (598–608 s) with QRS morphology changes due to axis shift with influence

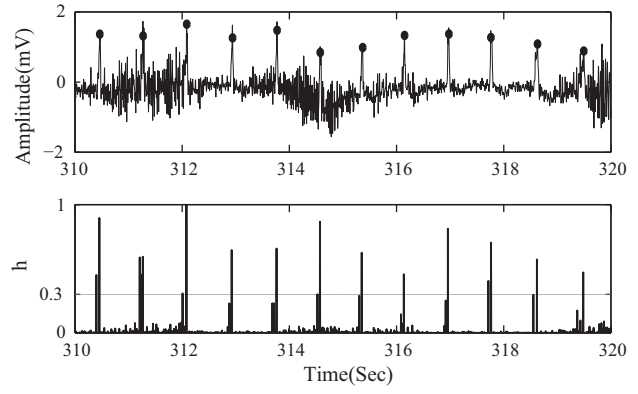

Fig. 9 – Plots of ECG waveforms and R peaks localization for MITDB record. 104: 310–320 s with muscle artifacts.

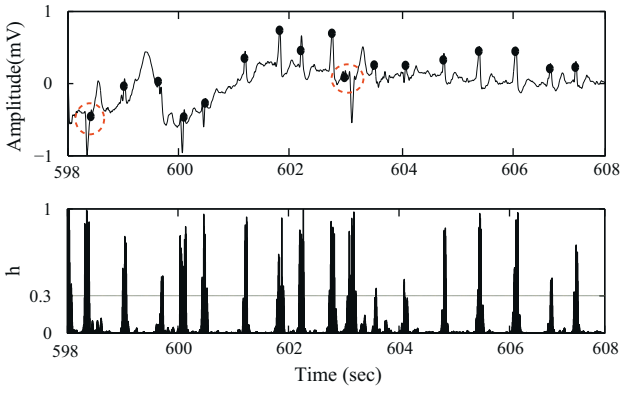

Fig. 11 – Plots of ECG waveforms and R peaks localization for MITDB record. 203: 398–608 s with muscle artifacts.

Table 2 – Comparison with other algorithms.

Method	S_e (%)	P_+ (%)	Er (%)
Our algorithm	99.64	99.82	0.54
J. Pan et al. (1985)	99.75	99.54	0.71
S. Choi et al. (2010)	99.66	99.80	0.54
Chen et al. [14]	99.47	99.54	0.98

of muscle artifacts, baseline drift and PVC beats followed by tall T waves is shown in Fig. 11. The effect of all these complicated patterns is attenuated when considering the parameter of QRS localization h. One can see that using a unique threshold $\lambda = 0.3 * \max(h)$, all QRS complexes are correctly localized except for the encircled R positions slightly shifted within less than 100 ms from the annotated time.

Statistical parameters are also used to compare detection algorithms. The sensitivity S_e, positive predictivity P_+ and error rate E_r, defined respectively as:

- $S_e = \frac{TP}{TP+FN}$
- $P_+ = \frac{TP}{TP+FP}$
- $E_r = \frac{FN+FP}{TB}$

Table 3 – The experimental results.

Rec	TB	TP	FP	FN	S_e (%)	P_+ (%)	Er (%)
100	2273	2273	0	0	100.00	100.00	0.00
101	1865	1864	2	1	99.95	99.89	0.16
102	2187	2185	0	2	99.91	100.00	0.09
103	2084	2084	0	0	100.00	100.00	0.00
104	2229	2211	12	18	99.19	99.46	1.35
105	2572	2528	15	44	98.29	99.41	2.29
106	2027	2027	8	0	100.00	99.61	0.39
107	2137	2134	4	3	99.86	99.81	0.33
108	1763	1728	25	35	98.01	98.57	3.40
109	2532	2532	0	0	100.00	100.00	0.00
111	2124	2122	0	2	99.91	100.00	0.09
112	2539	2537	0	2	99.92	100.00	0.08
113	1795	1793	1	2	99.89	99.94	0.17
114	1879	1875	1	4	99.79	99.95	0.27
115	1953	1953	0	0	100.00	100.00	0.00
116	2412	2397	4	15	99.38	99.83	0.79
117	1535	1535	0	0	100.00	100.00	0.00
118	2278	2273	0	5	99.78	100.00	0.22
119	1987	1987	0	0	100.00	100.00	0.00
121	1863	1861	1	2	99.89	99.95	0.16
122	2476	2476	0	0	100.00	100.00	0.00
123	1518	1518	0	0	100.00	100.00	0.00
124	1619	1619	1	0	100.00	99.94	0.06
200	2601	2586	11	15	99.42	99.58	1.00
201	1963	1938	7	25	98.73	99.64	1.63
202	2136	2135	1	1	99.95	99.95	0.09
203	2980	2944	25	36	98.79	99.16	2.05
205	2656	2643	0	13	99.51	100.00	0.49
207	1860	1848	8	12	99.35	99.57	1.08
208	2955	2930	5	25	99.15	99.83	1.02
209	3005	3004	1	1	99.97	99.97	0.07
210	2650	2627	18	23	99.13	99.32	1.55
212	2748	2748	0	0	100.00	100.00	0.00
213	3251	3250	0	1	99.97	100.00	0.03
214	2262	2257	2	5	99.78	99.91	0.31
215	3363	3353	4	10	99.70	99.88	0.42
217	2208	2203	2	5	99.77	99.91	0.32
219	2154	2154	0	0	100.00	100.00	0.00
220	2048	2048	1	0	100.00	99.95	0.05
221	2427	2424	1	3	99.88	99.96	0.16
222	2483	2481	2	2	99.92	99.92	0.16
223	2605	2604	0	1	99.96	100.00	0.04
228	2053	1996	27	57	97.22	98.67	4.09
230	2256	2255	3	1	99.96	99.87	0.18
231	1571	1571	0	0	100.00	100.00	0.00
232	1780	1779	0	1	99.94	100.00	0.06
233	3079	3066	0	13	99.58	100.00	0.42
234	2753	2745	1	8	99.71	99.96	0.33
All	109,494	109,101	193	393	99.64	99.82	0.54

where *TP* is the correctly detected beats (True Positive), *FP* is falsely detected beats (False Positive), *FN* is the undetected beats (False Negative) and *TB* the total analyzed beats. The sensitivity is used for evaluating the ability of the algorithm to detect true beats, the positive predictivity is used for evaluating the ability of the algorithm to discriminate between true and false beats and the error rate is used for evaluating the accuracy of the algorithm. These measures are determined by the decision-making rule that a beat is true when it is detected within 100 ms from the annotated time for each record, otherwise it is false [13]. The interval of 100 ms was mentioned as wider margin such that mentioned in [13]. In our application, the majority of detected R peaks are detected very closely or exactly corresponding to annotated times, some R peaks are shifted but less than 100 ms from the annotated times. The achieved results reported in Table 3 show statistical indices higher than or comparable to those cited in literature (see Table 2). Our algorithm succeeded in detecting correctly 99.46% of total beats, further, the sensitivity and the positive predictivity are $S_e = 99.64\%$ and $P_+ = 99.82\%$. Some record (105, 108, 201, 203 and 228) leading to an error rate higher than 2% suffer from changes in signal quality, baseline shifts, artifacts and QRS waves with highly unusual morphologies. The majority of algorithms found in literature obtained lower accuracy with these records.

4. Conclusion

In this paper, R peak detection algorithm based on QRS spectrum is proposed and tested with respect to the MIT-BIH arrhythmia database. Further, the possibility of detecting R positions of great variations of normal and abnormal QRS complex with influence of many artifacts is investigated. In this work we pointed out the advantage of using discreet wavelet transform considering energy levels where normal and abnormal beats are more pertinent. The importance of using details d_4 and d_5 is highlighted; the frequency range (5.62–22.5 Hz) take into consideration both normal and abnormal beats while the effect of different artifacts, T and P waves are attenuated eliminating the requirement of any preprocessing. Note that the majority of beats are detected with the initial threshold, making the algorithm simpler and less time consuming.

Conflict of interest statement

There is no conflict of interest to be declared.

REFERENCES

[1] B. Köhler, C. Hennig, R. Orglmeister, The principles of software QRS detection, IEEE Eng. Med. Biol. 21 (1) (2002) 42–57.
[2] J. Pan, W.J. Tompkins, A real-time QRS detection algorithm, IEEE Trans. Biomed. Eng. 32 (3) (1985) 230–236.
[3] P.S. Hamilton, W.J. Tompkins, Quantitative investigation of QRS detection rule using the MIT/BIH arrhythmia database, IEEE Trans. Biomed. Eng. 33 (12) (1986) 1157–1165.
[4] N. Arzeno, Zhi-De-Deng, C. Poon, Analysis of first-derivative based QRS detection algorithms, IEEE Trans. Biomed. Eng. 55 (2) (2008) 478–484.
[5] S. Choi, M. Adnane, G.J. Lee, H. Jang, Z. Jiang, H.K. Park, Development of ECG beat segmentation method by combining lowpass filter and irregular R-R interval checkup strategy, EXPERT Syst. Appl. 37 (7) (2010) 5208–5218.
[6] Q. Xue, Y.H. Hu, J. Tompkins, Neural-network-based adaptive matched filtering for QRS detection, IEEE Trans. Biomed. Eng. 39 (4) (1992) 317–329.
[7] S.S. Mehta, N.S. Ligayat, Comparative study of QRS detection in single lead and 12-lead ECG based on entropy and combined entropy criteria using Support Vector Machine, J. Theoretical Appl. Inform. Technol. 3 (2) (2007) 8–18.
[8] R. Poli, S. Cagnoni, G. Valli, Genetic design of optimum linear and nonlinear QRS detectors, IEEE Trans. Biomed. Eng. 42 (11) (1995) 1137–1141.
[9] G. Ruchita, A.K. Sharma, Detection of QRS complexs of ECG recording based on wavelet transform using Matlab, Int. J. Eng. Sci. 2 (7) (2010) 3038–3044.
[10] A.N. Dinh, D.K. Kumar, N.D. Pah, P. Burton, Wavelet for QRS detection, Engineering in Medicine and Biology Society, 23rd Conference of IEEE. (2002) 1883–1887.
[11] R. Mark, G.Moody, MIT-BIH arrhythmia database, <http://www.physionet.org/physiobank/database/mitdb/> (accessed on 12.07.11).
[12] N.V. Thakor, J.G. Webstor, W.J. Thompkins, Estimation of the QRS complex power spectra for design of a QRS filter, IEEE Trans. Biomed. Eng. 31 (11) (1984) 702–706.
[13] C. Meyer, J.F. Gavela, M. Harris, Combining algorithms in automatic detection of QRS complexes in ECG signals, IEEE Trans. Inf. Technol. B 10 (3) (2006) 468–475.
[14] S.W. Chen, C.H. Chen, H.L. Chan, A real-time QRS method based on moving-averaging incorporating with wavelet denoising, Comput. Method. Program. Biomed. 82 (3) (2006) 187–195.